5-2016

E56H + E59H Mutation affects binding of the recombinant *Haemphilus influenza* carbonic anhydrase to a Ni-NTA Column

Eric D. Lebel
Stanford University

Kathleen Cornely
Providence College, kcornely@providence.edu

E56H + E59H Mutation affects binding of the recombinant *Haemphilus influenza* carbonic anhydrase to a Ni-NTA Column

Eric D. Lebel[2] and Kathleen Cornely[1]
[1]*Department of Chemistry and Biochemistry, Providence College, Providence, RI 02918*
[2]*Department of Earth System Science, Stanford University, Stanford, CA 94305*

The *Haemophilus influenzae* carbonic anhydrase (HICA) is important in converting carbon dioxide to bicarbonate in bacteria. Endogenous cellular proteins, like *Escherichia coli* carbonic anhydrase (ECCA), have been observed to bind to a Ni-NTA column, which can be used as a means of protein purification. The possibility exists that proteins that do not normally bind to Ni-NTA, like HICA, can be engineered using site directed mutagenesis to introduce histidine residues that would give the protein the capability to bind, allowing for a one-step purification method. Site-directed mutagenesis was used to introduce the double mutation of E56H + E59H to *H. influenzae* carbonic anhydrase encoded on a plasmid. This protein was overexpressed in competent cells. A cell lysate was run on a Ni-NTA column to see how well the recombinant protein was able to bind to the column. We found that the E56H + E59H recombinant enzyme bound loosely to the column, and while most of the protein eluted in 10 and 25 mM washes with imidazole, some of the protein remained bound and was eluted with concentrations of imidazole between 25 and 250 mM. Therefore, the arrangement of surface histidine residues in the E56H + E59H mutant allowed some of the recombinant enzyme to bind loosely to Ni-NTA.

Carbonic anhydrases (EC 4.2.1.1) are important metalloenzymes that function in catalyzing the conversion of carbon dioxide to bicarbonate by hydration (1):

$$CO_2 + H_2O \rightleftharpoons HCO_3^- + H^+$$

To date, there are five known classes of carbonic anhydrases, designated as α-, β-, γ-, δ-, and ζ-carbonic anhydrases (2). The various forms of carbonic anhydrases have convergently evolved to use metals in their active sites, although none uses nickel (3). A variety of metals can be found in the active site of these metalloenzymes, including Fe(II), Zn(II), Co(II), and Cd(II). The most prevalent is Zn(II), and is especially important in β-carbonic anhydrases (4).

β-carbonic anhydrases have crucial roles in the photosynthesis of cyanobacteria (5). β-carbonic anhydrase is found in eubacteria, plant chloroplasts, red and green algae, and in the Archea (3). The activity of β-carbonic anhydrases is also important to ensure that there are adequate levels of CO_2 and HCO_3^- for other enzymes to function (5). Two of the primary β-carbonic anhydrases are *Haemophilus influenzae* carbonic anhydrase (HICA) and *Escherichia coli* carbonic anhydrase (ECCA).

Physiologically, carbonic anhydrases play an important role in regulating the functions of *Haemophilus influenzae* and *Escherichia coli* bacteria. The function of non-typal *Haemophilus influenzae* is regulated by the concentrations of CO_2 in the bloodstream. The bacteria are able to become resistant to penicillin and erythromycin, and *H. influenzae b* is able to invade epithelial cells only with supplemental carbon dioxide (6). Carbonic anhydrases can ensure that the virus has the appropriate concentrations of carbon dioxide to invade these cells. Additionally, β-carbonic anhydrase is essential for *E. coli* bacteria to survive in air and if the atmospheric partial pressure of CO_2 is high during anaerobic conditions (7). It is also believed that β-carbonic anhydrase is a necessary enzyme in bacteria for carboxylases involved in fatty acid synthesis (4).

The fundamental structural unit of β-carbonic anhydrases is a dimer. In HICA, the fundamental dimer is composed of two identical protein chains. These dimers form dimers of themselves, creating an overall tetrameric form (8). Specifically, the β-carbonic anhydrases have a horizontal plane of dimerization and a vertical plane of tetramerization.

The common structural element of β-carbonic anhydrases is a central parallel β-sheet that is composed of four strands (8). Most carbonic anhydrases use zinc as their coordination metal, and β-carbonic anhydrases have one zinc per monomer (8).

HICA and ECCA are both classified as type II β-carbonic anhydrases, as determined by their ability to adopt a structure that zinc-bound water molecule in the active site can be displaced by an Asp residue (1). The zinc ion in the active site is coordinated to 4 residues – Cys42, Asp44, His98, and Cys101 (8). Type II β-carbonic anhydrases also lack hydrogen bond donors that can interact with the bicarbonate ion that is bound in the position occupied by Asp44 (in HICA). Finally, the active site of Type II β-carbonic anhydrases lies along the dimer interface (8).

One of the current methods currently being investigated as a means to purify proteins is a one-step purification using a nickel nitrilotriacetic acid (Ni-NTA) column (9). Previous work has shown that a protein tag that included a structure of six histidine residues would be sufficient to bind to a Ni-NTA column using immobilized-metal affinity chromatography (IMAC); however, a protein tag can have the unwanted side effect of modifying the function of the protein (10). The current model of IMAC using a Ni-NTA column is that the nickel interacts with two histidine residues in a His-tag of a protein. These residues have one histidine residue between them (9). The most common way to elute the proteins that bind to the column is by elution with imidazole, which protonates the imidazole ring on the histidine residues, releasing them from the column (11).

While HICA and ECCA are very similar in structure, ECCA is able to bind to a Ni-NTA column so tightly that imidazole concentrations of 250-500 mM are needed for its elution, whereas wild-type HICA is unable to bind (3). ECCA is able to bind to the Ni-NTA column because of its cluster of histidines. It has six residues that are near each other, separated by distances between 5 and 7 Å (3). Previous work by Hoffmann *et al.* has shown that the mutation R160H in HICA causes the formation of a cluster of histidine residues similar to those present on ECCA (3). As a result, the mutant protein is able to bind to a Ni-NTA column and be eluted at imidazole concentrations of 190 mM (3). It is possible that other mutations can also be engineered to create a histidine residue cluster that would allow a mutant HICA protein to bind to a Ni-NTA column without affecting the function of the protein.

Here we report the construction of the E56H + E59H HICA mutant and its ability to bind to a Ni-NTA column. We chose this specific mutant because the mutation was on the surface of the protein and created a cluster of four histidine residues. Additionally, the mutation did not interfere with the active site of the enzyme. We felt that there was a strong chance that this mutation would exhibit qualities that would allow it to bind to a Ni-NTA column, which would allow for one-step purification of the protein.

EXPERIMENTAL PROCEDURES

Culture preparation – E. coli bacterial cells containing the HICA plasmid were obtained from transformed DH5α cells provided by Dr. Katherine Hoffmann's lab at Gonzaga University. These cells were grown on LB agar plates (1% tryptone, 0.5% yeast extract, and 1% NaCl) with 100 μg/mL ampicillin. These plates were streaked and left in the incubator for 54 hours at 37°C. A single colony was selected from the plate and inoculated in 5 mL of a liquid LB medium that contained 100 μg/mL ampicillin. The liquid culture grew for 18 hours overnight with agitation in a 37°C incubator.

Plasmid mini-prep – The Zyppy Plasmid Miniprep Kit (Zymo Research Corp) was used to isolate and purify the plasmid. Instructions from this kit were used with the following exceptions: 3 mL of the liquid culture were used in the mini-prep and centrifuged for 30 seconds at 20,000 × g to pellet the cells. The solution was decanted and the cells were resuspended in 600 μL of deionized water. The cells were lysed, neutralized, and then centrifuged at 15,000 × g for 3 minutes. The instructions from the kit were followed to elute the plasmid from the column. In order to increase yield, the column was incubated with 30 μL of elution buffer, or TE (10 mM Tris, 1 mM EDTA, pH=8) for 20 minutes at room temperature prior to elution. The final concentration of the plasmid was determined to be 69.8 ng/μL using the NanoDrop 1000 Spectrophotometer (Thermo Scientific).

Construction of the mutant E56H + E59H – The plasmid pHICA was used as a template to introduce the mutations through PCR. The primer 5'-TACAAAAAGATGGCCCGGATGAAGAT-3'

was used to introduce the actual mutations, and the underlined nucleotides indicate the codons that represent the mutated histidines. This reverse primer was used in the first round of PCR (designed to amplify the portion of the carbonic anhydrase gene containing the mutation) with the forward primer PhiQC, which has the sequence 5'-CACTGCATAATTCGTCTCGCTCAAGG-3'. The first round of PCR was designed to introduce the histidine mutants into the enzyme. The PCR reaction mixture contained 1 pmol/µL of both the reverse primer and PhiQC, 0.2 mM of dNTP mix, 20% v/v HF buffer, and 2.8 ng/µL of isolated plasmid from the mini-prep, diluted in nuclease-free water. Before PCR was run, 0.04 U/µL of Pfu Ultra DNA polymerase was added. All reagents were purchased from Thermo Scientific. A touchdown PCR protocol was used, which is 2 minutes at 95°C for the initial denaturation, 40 cycles of 30 seconds at 95°C, 30 seconds at 65°C, lowering by 0.5°C/cycle, and 30 seconds at 72°C. The final extension was 72°C for 10 minutes (12). To run a gel on the PCR product, a 1% agarose gel was prepared using TAE (40 mM Tris acetate, 1 mM EDTA, pH 8.5) and 0.01% v/v of SYBR Safe DNA Gel Stain (Life Technologies). A 100 bp DNA ladder (New England BioLabs) was used. The PCR product was excised from the gel and the DNA was recovered using the Zymoclean DNA Gel Recovery Kit (Zymo Research Corp). The instructions from the kit were followed. The DNA was eluted in 6 µL of TE elution buffer (10 mM Tris, 1 mM EDTA, pH=8) at room temperature.

The second round of PCR was designed to amplify the entire gene. The forward primer was a megaprimer, which was the DNA fragment that was purified in the preceding round of PCR (13). The reverse primer was Phi2X, which has the sequence:
5'-AGCTTGCATGCCTGCAGTTATTATG-3'.
The components of the PCR included 2.8 ng/µL of pHICA template, 1 pmol/µL of Phi2X primer, 18% v/v of the purified megaprimer, 0.2 mM of dNTP, 20% v/v of HF buffer, diluted with nuclease free water, and then 0.04 U/µL of Pfu Ultra polymerase was added. The touchdown PCR protocol was used again, except this time the extension time for each cycle was 1 minute instead of 30 seconds. The gel was prepared and run in the same manner as the first round of PCR. The expected length of the product was approximately 785 bp, and there was DNA of this approximate length present in the gel. This band was excised and purified using the Zymoclean DNA Gel Recovery Kit (Zymo Research Corp).

The third and final round of PCR was intended to replicate the entire mutant plasmid using Megaprimer Quikchange MegaWHOP PCR (13). The DNA fragment from the previous round of PCR was used as the only primer for this round of PCR, since the plasmid is circular. The components in the PCR mix include 2.8 ng/µL of the pHICA template, 20% v/v of the megaprimer that was isolated from the previous round of PCR, 0.2 mM of dNTP mix, 20% v/v of HF buffer, and this was all diluted in nuclease free water, then 0.04 U/µL of Pfu Ultra polymerase was added. The protocol for the thermocycler began with 2 minutes at 95°C for the initial denaturation, 30 cycles of 1 minute at 95°C, 1 minute at 65°C, lowering by 0.5°C/cycle, and 5 minutes at 72°C. The final extension was 72°C for 10 minutes. A 0.8% agarose gel was prepared and run to confirm that this round of PCR was successful, and a faint band was present at 5 kb, which is the expected plasmid length.

The PCR product was treated with 20 U of the restriction enzyme DpnI (New England Biolabs), which degraded the methylated parent plasmid, and left the mutated plasmid. The plasmid was incubated for 2 hours at 37°C and 5% v/v of the treated plasmid was combined with DH5α competent Premade Mix & Go *E. Coli* Cells (Zymo Research Corp) and left to incubate on ice for 40 minutes. The cells were plated on LB agar plates with 1 µg/mL ampicillin. The plates were left to grow overnight. The next day, a colony was inoculated in 5 mL of LB media with 100 µg/mL ampicillin, as previously described. A plasmid mini-prep was performed for each of the three cultures as previously described. The sample was eluted with 15 µL of elution buffer at room temperature, and then it was sent to the Massachusetts General Hospital (MGH) Facility for sequencing. The samples were prepared using their instructions, except each sample only contained between 30-40 ng/µL of plasmid, as determined by using the NanoDrop 1000 Spectrophotometer (Thermo Scientific). Each sample also contained 1.5 µM of pRRX forward sequencing primer which has the sequence: 5'-GGCTCGTATAATGTGTGGAATTG-3'.

Cell transformation – A liquid culture was grown in 5 mL of LB media with 100 µg/mL ampicillin as previously described. The next day, a mini-

prep was performed on this cell culture as previously described. The DNA was eluted in 6 µL of elution buffer that was warmed to 48°C. The plasmid was transformed in XJb cells using Premade Mix & Go Competent *E. Coli* Cells (Zymo Research Corp) and the manufacturer's instructions were followed. The cells were incubated on ice for 45 minutes, then spread on LB agar plates with 100 µg/mL ampicillin, which were incubated at 37°C overnight. Overnight liquid cultures in 5 mL of LB media with 1 µg/mL ampicillin were made for two of the colonies. The cultures were combined and the cells were pelleted by centrifuging the media at 8000 × g for 5 minutes. The cells were resuspended in 10 mL of fresh LB media with 100 µg/mL ampicillin. A 1 liter overexpression culture was made using TB medium, which is 90% v/v TB nutrient (27.2 % tryptone, 60% yeast extract, and 4.4% glycerol) and 10% v/v TB buffer ($H_2PO_4^-/HPO_4^{2-}$ buffer, pH 7.84 and formal concentration 0.89 M) pre-warmed to 37°C. The media was combined in a 2.5 L Tunair flask, along with 100 µg/mL of ampicillin and 3 mM arabinose. The entire contents (10 mL) from the centrifugation mixture containing the transformed cells were placed in the overexpression medium. The culture was inoculated at 37°C for 3 hours, and when the absorbance at 600 nm was ~0.8, 0.20 mM IPTG (isopropyl-β-D-thiogalactopyranoside) was added. The cells were incubated at 37°C with vigorous shaking for 36 hours. The cells were harvested by centrifugation at 6,500 × g for 10 minutes and subsequently frozen at -80°C.

Cell lysis – The cells were removed and thawed from the freezer and resuspended in 3 mL/g of extraction buffer (10 mM Tris, 1 mM EDTA). One-half of a Protease Inhibitor Mini Tablet without EDTA (Thermo Scientific) was added to the sample. The mixture was placed on the 37°C shaker with vigorous shaking for one hour, and 20 U of DNAse I (New England BioLabs) was added to the sample after 30 and 45 minutes of incubation. The sample was centrifuged for 30 minutes at 35,000 × g and the pellet was discarded. The supernatant was centrifuged for 15 additional minutes at 35,000 × g. A BCA Assay was performed using a BSA kit (Thermo Scientific) to determine the concentration of the protein (14).

Ni-NTA Chromatography – About 0.5mL of Ni-NTA bed volume (Qiagen) was prepared with 2 mL of extraction buffer (10 mM Tris, 1 mM EDTA) and 10 mM of imidazole, to which 4 mL of cleared lysate was added. This mixture was shaken at 4°C for 60 minutes, then loaded onto a column. The flow-through was collected, and the sample was washed once with 2.5 mL of 10 mM imidazole, once with 2.5 mL of 25 mM imidazole, and eluted 4 times with 0.5 mL of 250 mM imidazole and 4 times with 0.5 mL of 500 mM imidazole. The absorbance of each of these samples was measured using the Carey-50 at 280 nm. An SDS-PAGE gel was run according to the specifications of Laemmli (15), except the separating gel consisted of 10% acrylamide, 0.27% bis-acrylamide, 0.375 M Tris, 0.1% SDS at pH 8.8. The stacking gel consisted of 0.3% acrylamide, 0.08% bis-acrylamide, 0.125 M Tris, and 0.1% SDS at pH 6.8. The polymerization of both gels was stimulated by adding 0.003% ammonium persulfate and 0.00025% v/v of tetramethylethylenediamine (TEMED). To prepare each of the samples, 1% v/v of β-mercaptoethanol was added to each sample with Laemmli sample buffer (0.063 M Tris, 10% glycerol, 2 mM DTT, and 2.3% SDS at pH 6.8). Approximately 60 µL of sample and buffer were loaded into each well. The samples were heated at 100°C for two minutes before being loaded onto the polymerized gel. A BenchMark pre-stained protein ladder (Life Technologies) was also loaded onto the gel. The wells were filled with a Tris/glycine buffer (25 mM Tris, 0.192 M glycine, 0.1% SDS at pH 8.3). The gel was run for a total of 5 hours at 55 mamps through the stacking gel and 30 mamps through the separating gel. A Coomassie blue staining solution (40% methanol, 7% acetic acid) was used to stain the gel overnight. A destaining solution (15% methanol, 7.5% acetic acid, 3% glycerol) was used to destain the gel, and was changed twice in two days. The gel was dried at 80°C under a vacuum for 2 hours.

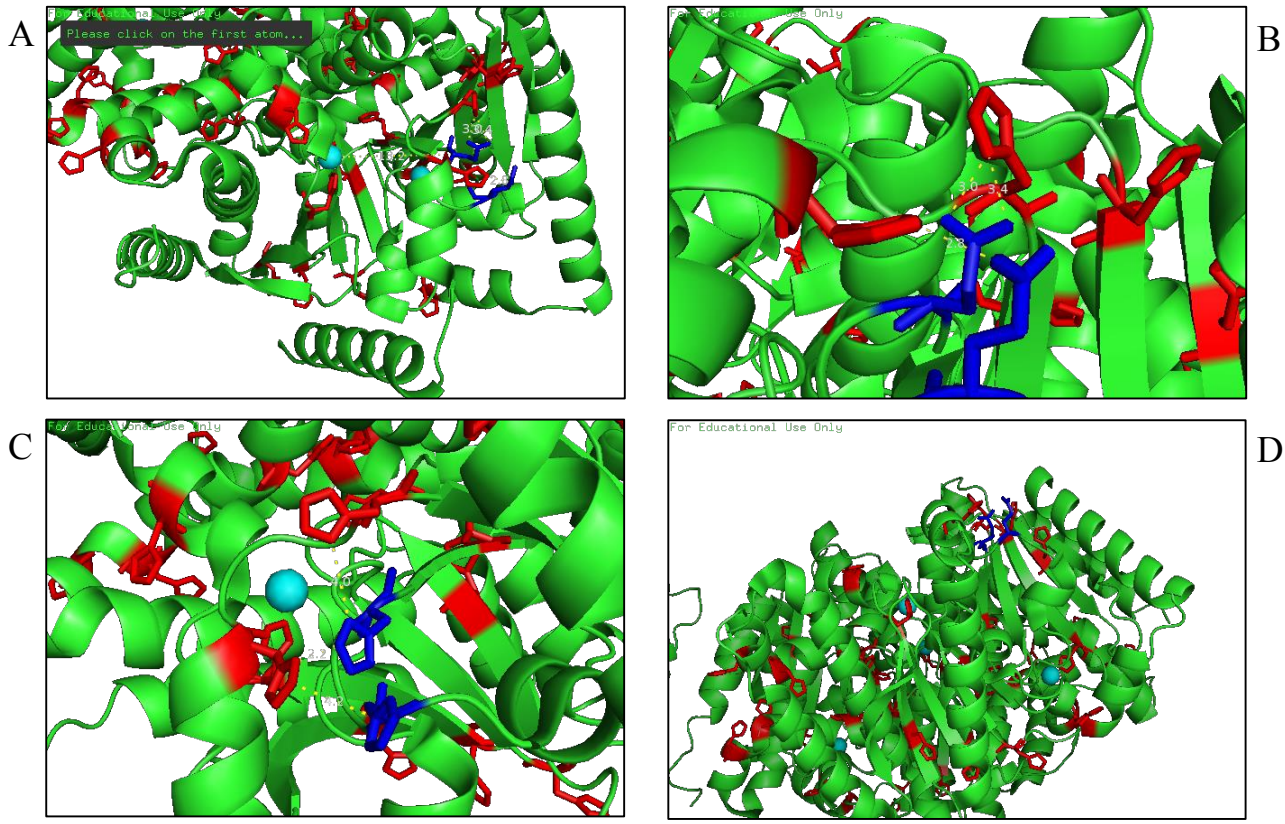

FIGURE 1. **PyMol images visualize the E56H + E59H mutation on the HICA protein.** Panel A shows an overview of the targeted glutamic acid residues, in blue, and all the histidine residues in red. They are in close proximity to the surface of the protein yet still far enough away from the active site. Panel B shows the targeted glutamic acid residues and the surrounding histidine amino acids. Panel C shows a similar view, except the glutamic acid residues are seen as histidines. The distances between each of the four histidine amino acids on the surface range from 2.8-7.2 Å. Panel D shows the whole HICA protein with the mutation in blue, and it can be seen that the targeted amino acids are on the surface of the protein to allow the cluster of histidines bind to the Ni-NTA column.

RESULTS

Characterization and synthesis of the E56H + E59H mutant – The specific E56H + E59H mutation was visualized using PyMol (Figure 1). The mutated residues created a cluster of four histidine amino acids that were present on the surface of the protein chain, and therefore could interact with the Ni-NTA. The two endogenous histidine residues were His31 and His35. The closest distance between the mutated residues and the Zn^{2+} active site was 13.2 Å. The distance separating the cluster of endogenous and mutated histidine residues ranged from 2.8 Å between the two closest residues and 7.2 Å between the two furthest residues.

The PCR products were recovered from the DNA gels that were run (Figure 2). The expected length of the PCR product after the first round of PCR was 356 bp, and a band at approximately 350 bp was present in the gel. The second round of PCR, which amplified the whole gene, had a band that was approximately 900 bp in length, which was close to the expected length of 785 bp for the amplified region. The gel was run after the final round of PCR that amplified the plasmid merely to verify that the PCR worked. A very faint band at 5 kbp could be seen on the gel, which was the expected length of the HICA plasmid.

To determine the concentration of the isolated protein, a BCA assay was run. The standard curve was used to determine the concentrations of the unknowns (Figure 3). A 20:1 diluted sample was used to fit in the range of the standard curve, and the concentration of protein in the original lysate was determined to be 4390 µg/mL ± 90 µg/mL.

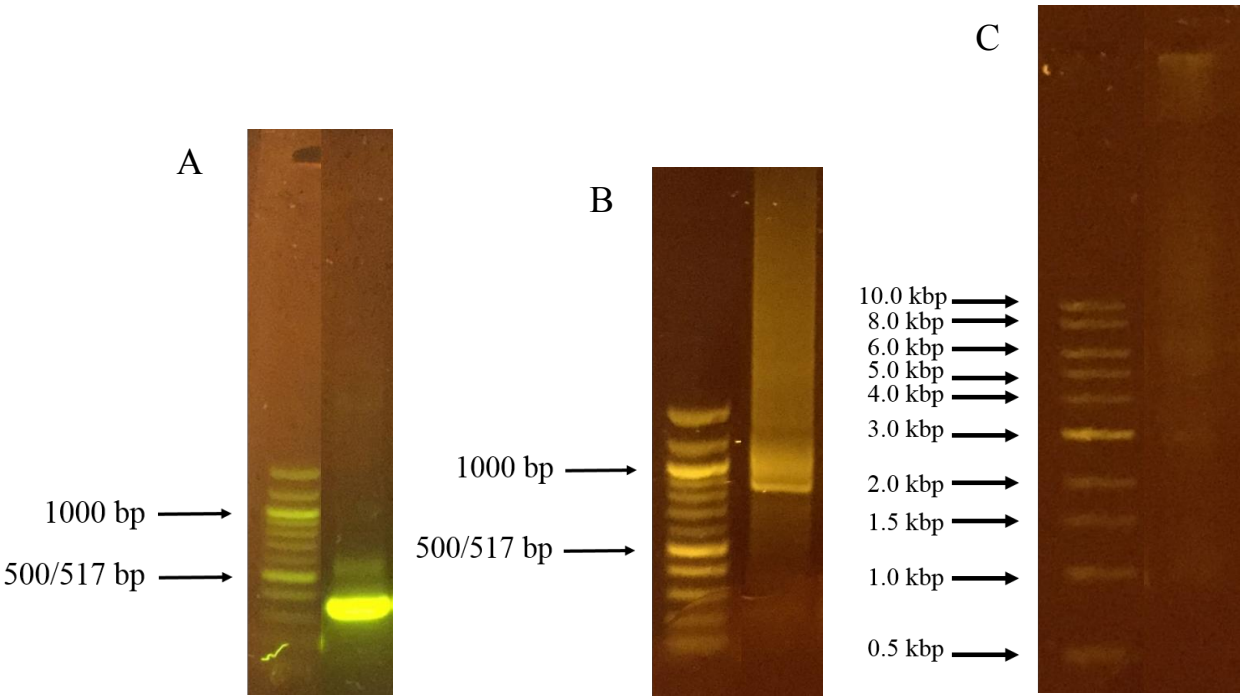

FIGURE 2. **DNA gels were run after each round of PCR.** Panel A shows the gel that was run after the preliminary round of PCR and a band is present at 300 bp. In Panel B, the entire gene was amplified using megaprimer PCR, and a band can be seen at 900 bp. Panel C shows the gel that was run after the entire plasmid was amplified. A very faint band is present at 5 kbp.

Immobilized-metal affinity chromatography using Ni-NTA – After the Ni-NTA column was run, the absorbances were taken of each of the fractions at 280 nm. The profile shows the relative concentrations of the proteins throughout the course of the washes and elutions at various concentrations of imidazole (Figure 4). The majority of the protein came off the column in the flow-through and also in the early washes. Some protein eluted at 250 mM imidazole, as can be seen by the moderate peak present over these fractions. Hardly any protein came off the column during the 500 mM elution, since the absorbances remained low.

The HICA should be present on the SDS-PAGE gel (Figure 5) at approximately 27 kDa. Proteins of this molecular weight or less were present with the dye at the bottom of the gel, since the gel was only 10% acrylamide. The darker bands indicate that more HICA was present at the various stages of washing and elution. Moreover, it is possible that HICA formed dimers, as can be seen by the very faint bands present at approximately 55 kDa. It can be seen that most of the HICA was present in the flow-through and in the early washes, but small amounts were present for the 250 mM imidazole elution, and in even smaller amounts for the 500 mM imidazole elution.

DISCUSSION

The gels that were run after each round of PCR indicate that the PCR was successful. A band was present at the appropriate length based on the fragment that was being amplified. We confirmed the success of the PCR when the results from the MGH sequencing facility reported that one of the samples we prepared for sequencing did in fact have the appropriate mutation incorporated into the plasmid. After overexpressing the E56H + E59H mutant plasmid in competent cells in cell culture, the protein was isolated and its measured concentration of 4390 µg/mL ± 90 µg/mL is reasonable.

When run on a Ni-NTA column, the protein did not perform as expected. Although there was some evidence that it did bind slightly to the column, most of the HICA came off during the flow-through

or the wash with 10 mM imidazole. The little HICA that did come off during the elutions came off between 25 and 250 mM imidazole. However, it is likely that the mutant required a concentration of imidazole that was toward the lower end of this range, since the R160H mutant designed by Hoffmann *et al*. was eluted at 190 mM imidazole (3). The R160H mutant most closely resembles ECCA, which endogenously binds to a Ni-NTA column. This may be a result of there only being four histidines in the area of the cluster of histidines on the surface of the protein as opposed to the six in the R160H mutant (3). Perhaps introducing other mutant histidine residues in the area of the E56H + E59H mutations would add to this mutant's ability to bind to the Ni-NTA column.

When using IMAC with Ni-NTA, it is possible to overload the column with more mutant protein than can feasibly bind to the resin. However, it was not suspected that the column was overloaded. Approximately 30 mg of protein should have been able to bind to the 0.5 mL of resin in the column, and approximately 17.56 mg of protein was loaded onto the column. Only a fraction of the protein present was HICA, but even if all the protein present were HICA, the column still would not have been overloaded.

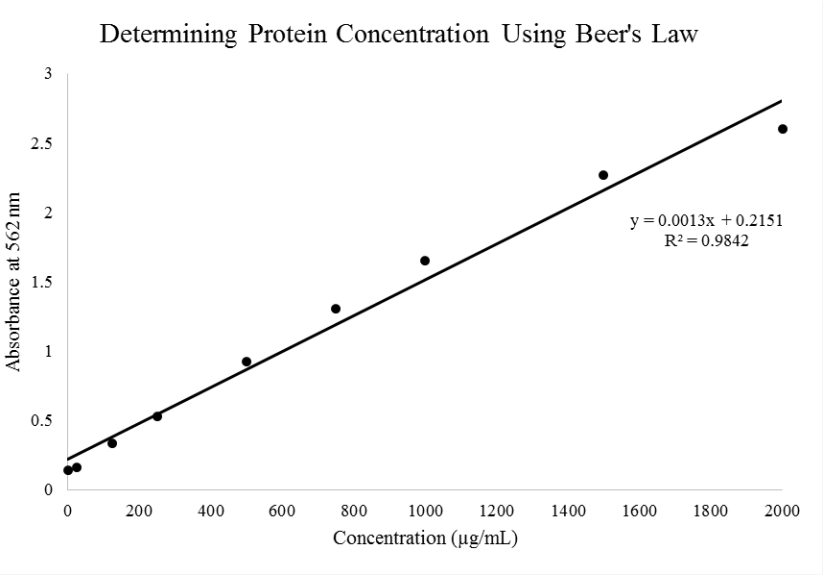

FIGURE 3. **The concentration of the extracted protein was measured using a BCA assay.** The standards of BSA were prepared and the absorbances were taken at 562 nm. A standard curve was plotted in order to determine the concentration of unknown samples of protein.

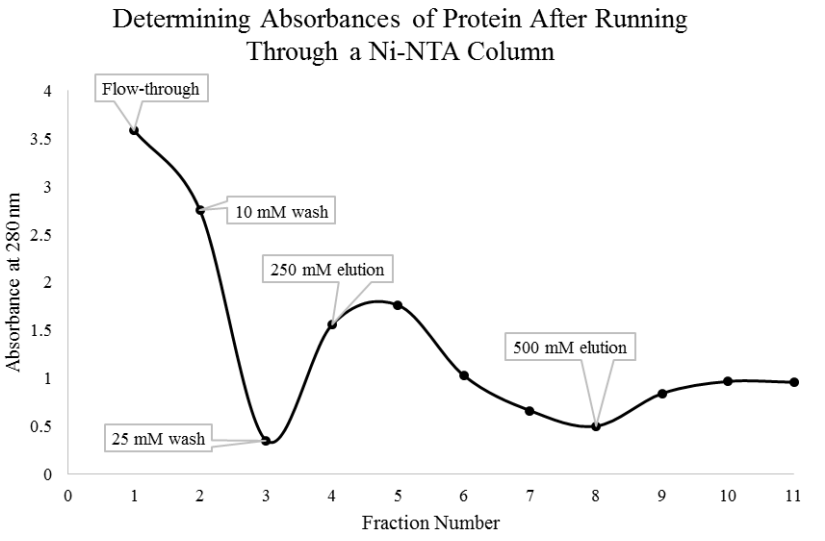

FIGURE 4. **Absorbances at 280 nm were taken of each of the fractions collected off of the Ni-NTA column.** Most of the protein came off the column in the flow-through. During the initial washes, much of the loosely bound protein also came off the column. A small amount of protein came off the column when it was eluted with 250 mM imidazole. Very little protein was eluted when 500 mM imidazole was run through the column.

It is important to note that the amount of sample (in grams of protein) that was added to each lane of the SDS-PAGE gel was normalized to ensure that approximately the same amount of protein was added to each lane. In addition, the HICA ran with the dye and elution front of the gel, so all proteins that were approximately 27 kDa or less would be present in this band, which may have created some inconsistencies in the results.

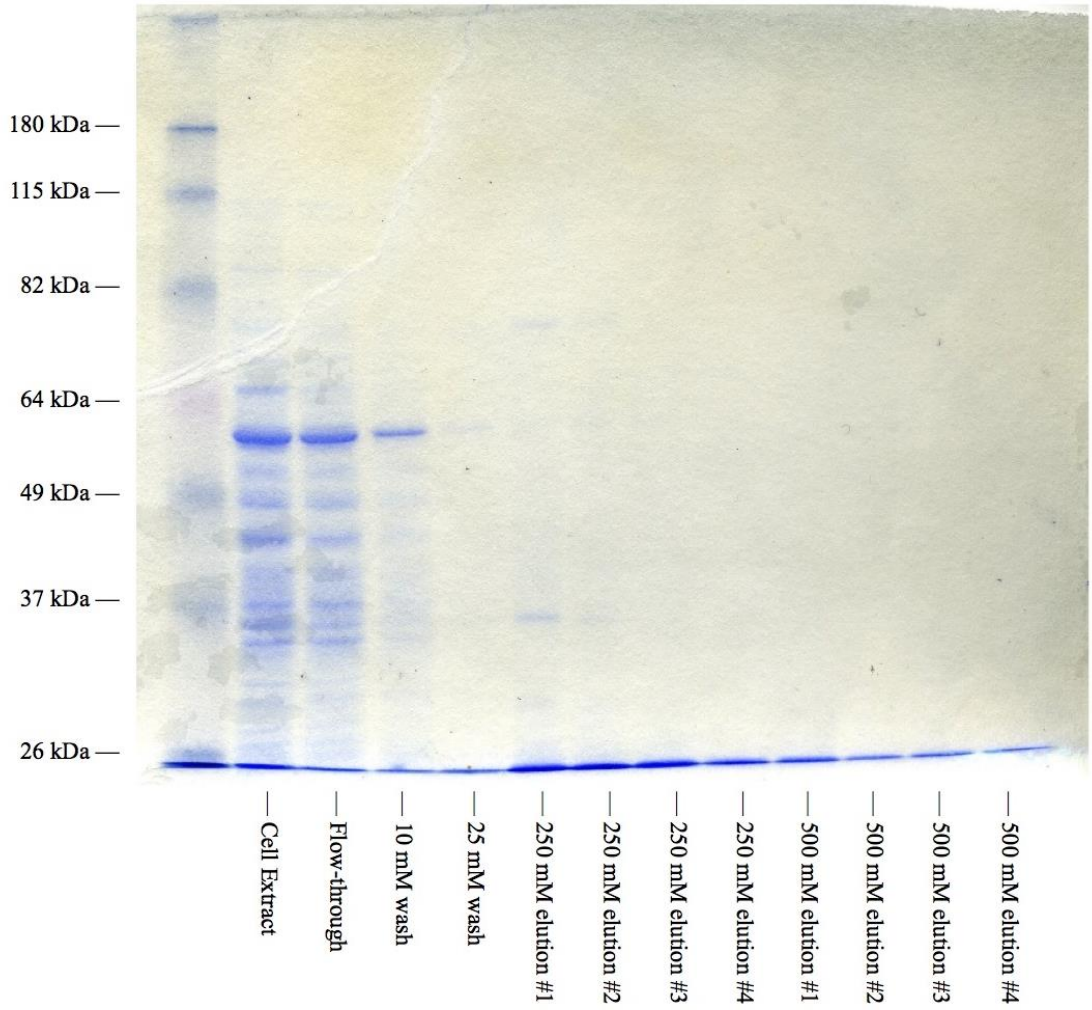

FIGURE 5. **A 10% acrylamide SDS-PAGE gel was run with each of the fractions that were collected from the Ni-NTA column.** The substances with the lowest molecular weight all ran with the dye since the concentration of the acrylamide was too low to resolve these species. The HICA band should be present at about 27 kDa, so it still can be seen at the very bottom of the gel. Much of the HICA came off with the flow-through and early washes. There was a small amount that was eluted with the 250 mM elution, and an even smaller amount came off the column during the 500 mM elution.

There are some drawbacks to this system of protein purification. For instance, the protein of interest is compromised by chelating groups, such as EDTA (16), but we did not add EDA to our mutant. Additionally, the His mutants do not always effectively remove the contaminant proteins (16). On the protein gel for the elutions, there are very faint bands visible at higher molecular weights. These bands could either be contaminants or dimers of the mutated HICA protein, especially at 55 kDa, which is the molecular weight of a HICA dimer. If the latter is the case for these bands, then it supports the conclusion that this method may be viable for purifying HICA.

The mutation E56H + E59H was chosen based on properties of the cluster of histidines that were formed. Since the mutations were far enough away from the active site, they did not interfere with the functioning of the enzyme. Kinetic and structural studies have shown that HICA and ECCA contain a noncatalytic binding site for the bicarbonate ion, and this is unique to these two enzymes (17). The bicarbonate is specifically surrounded by Trp39, Arg64, and Tyr181, and lies within 8 Å from the zinc active site and near the plane of dimerization.

Other residues that are near the active site include Cys42, Asp44, His98, and Cys101 (17). The mutated E56H + E59H and endogenous His31 and His35 residues do not interfere with the active site nor the noncatalytic bicarbonate binding site.

When designing this mutant, it was important to consider the effects of the mutation on the activity of the enzyme. Carbonic anhydrases are enzymes that react very quickly. When catalyzing the forward reaction, CO_2 is concentrated in the active site cleft with hydrophobic residues. The zinc metal binds a hydroxide ion and is oriented by an Asp residue, which attacks the CO_2. This attack converts the CO_2 into a bicarbonate ion, which is stabilized by hydrogen bonding to Gln151. Water then replaces the bicarbonate at the zinc ion and the final step involves the loss of a proton from this water to regenerate the hydroxide ion that is bound to the zinc (8). Crystal structures of each of the Type I and Type II β-carbonic anhydrases have shown that the structure of the R-state of Type II carbonic anhydrases resembles the structure of Type I carbonic anhydrases (18). This is because the binding of the bicarbonate ion causes an allosteric conformational change, and this is supported by the observation that the Type II carbonic anhydrases have cooperative pH-rate profiles and are cooperatively inhibited by the bicarbonate ion (18). It is imperative that this mutation does not interfere with either the active site or the binding site of the bicarbonate ion, as the bicarbonate is a very important allosteric regulator. The distance of the mutant from the active site, 13.2 Å, is great enough for the mutation to not affect the enzyme activity.

Additionally, like the R160H mutant engineered by Hoffmann *et al.,* (3) the mutated residues were on the surface of the protein so that they could affect its binding to the Ni-NTA column. Hoffmann *et al.* reported that the optimal distance between the histidine residues is 5 to 7 Å since this is the distance between histidines in the engineered R160H mutant (3). Hoffmann *et al.* also reported that the distances between histidine residues between the protein chains range from 3.5-4.5 Å (3). One of the major differences between the successful R160H mutant and the E56H + E59H mutant is that the R160H mutant is on the horizontal plane between the two dimers (3), but the E56H + E59H mutant is on the surface of the protein, far from any plane of dimerization. This prevents the histidine cluster from interacting with histidine residues on other chains. It has been found that the distances between the metal and its ligands in a nickel complex vary from 1.8 to 2.4 Å (11). The measured distances between the endogenous and mutated histidine residues in the E56H + E59H mutant fall within the range of 2.8 to 7.2 Å, which suggests that the mutant residues are not too closely spaced to impede their ability to bind to a Ni-NTA column.

Plans for future work on this project include obtaining kinetic data on the E56H + E59H mutant. Other mutants could be engineered that exhibit qualities that more closely resemble the R160H mutant and the His-tags that have been shown to be successful at binding to a Ni-NTA column (3).

Acknowledgements – We would like to thank Dr. Katherine Hoffman from Gonzaga University for helping with this project. KC acknowledges the Walsh fund that supported her travel to Gonzaga University for training. Additionally, we would like to thank the following people for their support of this project: Heloise Dubois and the Providence College Undergraduate Research Committee for funding a pilot study of this project, Nicanor Austriaco, Ph.D., O.P., Brett Pellock, PhD; and the Department of Chemistry and Biochemistry and the Department of Biology at Providence College.

REFERENCES

1. Rowlett, R. S., Hoffmann, K. M., Failing, H., Mysliwiec, M. M., and Samardzic, D. (2010) Evidence for a Bicarbonate "Escort" Site in *Haemophilus influenzae* β-carbonic anhydrase. *Biochemistry* **49,** 3640-3647
2. Supuran, C. (2011) Bacterial carbonic anhydrases as drug targets: toward novel antibiotics? *Front. Pharmacol.* **2:34,** 1-6
3. Hoffman, K. M., Wood, K. M., Labrum, A. D., *et al.* (2014) Surface histidine mutations for the metal affinity purification of a β-carbonic anhydrase. *Anal. Biochem.* **458,** 66-68
4. Hoffmann, K. M., Million-Perez, H. R., Merkhofer, R., *et al*. (2015) Allosteric Reversion of *Haemophilus influenzae β*-Carbonic anhydrase via a proline shift. *Biochemistry* **54,** 598-611
5. Cronk, J. D., Endrizzi, J. A., Cronk, M. R., *et al.* (2001) Crystal structure of *E. coli* β-carbonic anhydrase, an enzyme with an unusual pH-dependent activity. *Prot. Sci.* **10,** 911-922

6. Langereis, J. D., Zomer, A., Stunnenberg, H. G., et al. (2013) Nontypeable *Haemophilus influenzae* carbonic anhydrase is important for environmental and intracellular survival. *J. Bacteriol.* **195,** 2737-2746
7. Emameh, R. Z., Barker, H., Tolvanen, M. E. E., *et al.* (2014) Bioinformatic analysis of beta carbonic anhydrase sequences from protozoans and metazoans. *Biomed. Central.* **7:38,** 1-12
8. Rowlett, R. S. (2010) Structure and catalytic mechanism of the β-carbonic anhydrases. *Biochim. Biophys. Acta.* **1804,** 362-373
9. Block, H., Barbara, M., Spriestersbach, A., *et al.* (2009) Immobilized-Metal Affinity Chromatography (IMAC): A review. *Methods Enzymol.,* **463,** 439-473
10. Mooney, J. T., Fredericks, D., Christensen, T., and Hearn, M. T. W. (2014) Removal of cleavage slow points from affinity tags used in the IMAC purification of recombinant proteins. *J. Biotechnol.* **9,** 1023-1032
11. Balakrishnan, R., Ramasubbu, N., Varughese, K. I., and Parthasarathy, R. (1997) Crystal structures of the copper and nickel complexes of RNase A: Metal-induced interprotein interactions and identification of a novel copper binding motif. *Proc. Natl. Acad. Sci.* **94,** 9620-9625
12. Roux, K. H. and Hecker, K. H. (1997) One-step optimization using touchdown and stepdown PCR. *Methods Mol Bio* **67,** 39-45
13. Barik, S. (1996) Site-directed mutagenesis in vitro by megaprimer PCR. *Methods Mol. Bio.* **57,** 203-215
14. Smith, P. K., Krohn, R. I., Hermanson, G. T., *et al.* (1985) Measurement of protein using bicinchoninic acid. *Anal. Biochem.* **150,** 76-85
15. Laemmli, U. K. (1970) Cleavage of Structural Proteins during the Assembly of the head of bacteriophage T4 *Nature* **227,** 680-685
16. Keefe, A. D., Wilson, D. S., Seelig, B., and Szostak, J. W. (2001) One-step purification of recombinant proteins using a nanomolar-affinity streptavidin-binding peptide, the SBP-tag. *Academic Press* **23,** 440-446
17. Cronk, J. D., Rowlett, R. S., Zhang, K. Y. J., et al. (2006) Identification of a novel noncatalytic bicarbonate binding site in eubacterial β-carbonic anhydrase. *Biochemistry* **45,** 4351-4361
18. Rowlett, R. S., Tu, C., Lee, J., et al. (2009) Allosteric site variants of *Haemophilus influenzae* β-carbonic anhydrase. *Biochemistry* **48:26,** 6146-6156